

Presented at the Processing of Fibers & Composites Conference, Barga, Italy, May 22, 2000

HIGH PERFORMANCE OXIDE FIBERS FOR METAL AND CERAMIC COMPOSITES

D. M. Wilson and L. R. Visser

3M Specialty Fibers & Composites Program

St. Paul, MN, USA 55144-1000

Keywords

Fibers, Al₂O₃, mullite, microstructure

Summary

A family of oxide fibers, Nextel™ 610 Ceramic Oxide Fiber, Nextel™ 720 Ceramic Oxide Fiber and a new fiber, Nextel™ 650 Ceramic Oxide Fiber, has been developed specifically for the reinforcement of metal and ceramic matrix composites. This paper summarizes room and high temperature properties for these fibers. The strength of both single filaments and multi-filament rovings of Nextel 610, 650 and 720 fibers was determined between 25 and 250 mm gauge length. Weibull analysis was used to compare the statistical fracture distribution and gauge length dependence of strength. Fiber fracture statistics were in accord with Weibull theory; the effect of diameter variability on the statistical analysis was found to be small. Fractographic analysis on Nextel 610 fiber was used to identify primary fracture-causing defects; defect size was correlated with Griffith fracture predictions.

High temperature single filament strength measurements were performed on Nextel 610, 650 and 720 fibers between 800°C and 1400°C. High temperature strength

varied inversely with strain rate. In combination with tensile creep tests at 1100°C and 1200°C, these were used to compare the elevated temperature capability of each fiber and determine maximum use temperatures. The development of crystalline yttrium aluminum garnet (YAG) fibers that demonstrate further improvements in creep performance relative to Nextel 720 fibers is also discussed.

Introduction

Oxide fibers are traditionally considered to have lower strength and creep resistance than covalently bonded materials such as SiC. However, in the mid 90's, two new fibers, Nextel 610 fiber and Nextel 720 fiber, were developed that have uniquely high tensile strength and creep resistance. The high strength of Nextel 610 fiber (3.3 GPa) has allowed the development of a new generation of aluminum matrix composites that have tensile strength in excess of 1500 MPa¹. The creep resistance of Nextel 720 fiber^{2,3,4} allows the fabrication of oxidation-stable ceramic composites with useful load-bearing capability above 1100C^{5,6,7}. A new rare-earth doped alumina fiber, Nextel 650 fiber, has recently been developed that has 100 times lower creep rate than Nextel 610 fiber⁸. These fibers comprise a family of composite grade fibers specifically designed for the reinforcement of metal and high temperature ceramic matrix composites. One unique and critical difference between these fibers and other commercial fibers is that they are fully crystalline. Most commercial fibers contain silica or other non-crystalline phases, including the older NextelTM fibers such as NextelTM 312, 440 and 550 Ceramic Oxide Fibers. Amorphous phases become viscous at high temperatures, so are

detrimental to creep performance. Equally critical for fibers designed for composite reinforcement is the reactivity of amorphous phases compared with fully crystalline fibers. Crystalline fibers containing high amounts of α -Al₂O₃ that are free of glassy phases are very chemically stable. High chemical stability leads to good environmental stability in corrosive atmospheres, low reactivity with respect to metal matrixes such as aluminum, and less interaction with a variety of ceramic matrices. Several successful high temperature composites utilize porous oxide matrices^{5,7}. Porous oxide matrices promote crack deflection at fiber-matrix interfaces, leading to fiber debonding and pullout, thereby providing high composite toughness. This approach to composite design requires highly stable and non-reactive fibers to prevent strong matrix-fiber interactions. This type of composite, which does not require fiber coatings, is finding increasing application in part because of the significant cost advantages relative to other systems.

Nextel 720 fiber was developed for load-bearing applications at temperatures in excess of 1000C. The superior high temperature creep performance of Nextel 720 fiber results from a high content of mullite, which has much better creep resistance than alumina. Additionally, Nextel 720 fiber consists of 0.5 μ m globular grains of mullite; this is five times larger than grains in Nextel 610 fiber. In fine-grained oxides, the creep rate is inversely proportional to grain size. Lastly, the presence of acicular and globular grains of mullite and alumina reduces grain boundary sliding. However, these microstructural factors that improve creep represent a tradeoff with respect to strength. High strength fibers should preferably have a fine and uniform grain size. High contents of alumina, which has higher fracture toughness than mullite, are also advantageous for strength.

Nextel 650 fiber was recently developed for high temperature composite applications in which the presence of mullite and other silicon-containing phases is not desirable. Additional information on the microstructure and properties of Nextel 650 fibers was recently published⁸. Nextel 650 fibers were developed with the goal of producing a fiber with improved strength and chemical stability relative to Nextel 720 fibers with superior creep performance relative to Nextel 610 fibers. High alumina fibers are more corrosion resistant in many environments, such as those containing alkalis, than fibers containing silica. High pressure steam environments at temperatures above 1100C, such as in combustors in gas turbines, may also cause degradation in Nextel 720 fibers. Also, Nextel 720 fiber has a strength of only 2.1 GPa, significantly less than Nextel 610 fiber, as a result of its larger grain size. Harmer⁹ and others¹⁰ have reported that doping alumina with rare earth oxides such as Y_2O_3 reduces creep in alumina by 1 to 2 orders of magnitude. The use of Y_2O_3 to reduce diffusivity in Al_2O_3 oxidation scales formed on metal alloys is also well known¹¹. The reduction in creep is attributed to reduced grain boundary diffusivity caused by segregation of Y^{3+} to grain boundaries¹². Since creep in fine-grained alumina is controlled by diffusion-related phenomena on grain boundaries, e.g., diffusion, grain boundary sliding, and defect elimination, rare earth doping reduces the creep rate in alumina.

Experimental and Analytical Procedures

Single filament strength testing was performed by directly gripping fibers with rubber-faced clamp grips with 25 x 25 mm grip faces. For routine testing, a 25 mm

gauge length and a fiber loading rate of 0.02/min was used. Filament diameters were measured using a Measure-Rite image analysis system (Model M25-6002 Dolan-Jenner Industries, Lawrence, MA), attached to a light microscope at 1000X magnification. In this system, fibers were measured end-on relative to a round template. This method has a resolution of 0.3 μm and has been determined to be accurate to within 0.3 μm relative to SEM measurements.

For most single filament strength testing, filament diameter was not measured; average diameters were calculated from roving denier and the number of filaments, assumed to be 410 for 1500 denier rovings (denier = grams/9000m length). Calculated diameters were 11.52, 11.22 and 12.34 μm were used for 1500 denier Nextel 610, 650 and 720 fibers, respectively, and 11.98 μm for 3000 denier Nextel 610 roving (770 filaments/roving). The differences in diameter result from the different density of each fiber type.

The statistics of fiber fracture are commonly reported as a Weibull distribution. The application of Weibull theory to high modulus fibers has been reviewed¹³. The probability of failure of a material is given by:

$$P = 1 - \exp [-V/V_0(\sigma/\sigma_0)^m] \quad (1)$$

where m = Weibull modulus, V = gauge length, σ = failure strength and V_0, σ_0 = scaling constants. For a single gauge length, Equation 1 reduces to:

$$\ln(\ln(1/1-P)) = m \cdot \ln \sigma + k \quad (2)$$

where k is a constant. The Weibull modulus, m , is then determined graphically as the slope of the “Weibull plot” of $\ln(\ln(1/1-P))$ vs. $\ln \sigma$. For Weibull plots, $P = (i-0.5)/n$ was used to estimate fracture probability, where n is the number of fibers tested and i is the rank of strength for each fiber.

Another method of determining Weibull modulus is to measure fiber strength as a function of gauge length. With increasing gauge length, the chance of finding a large flaw increases, so fiber strength decreases. The effect of gauge length is given by the equation:

$$\ln \sigma = -1/m \ln L + k' \quad (3)$$

where L is gauge length and k' is a constant. Thus, the slope of a log-log plot of strength vs. gauge length is $-1/m$.

Fractography testing was performed by breaking fibers embedded in grease to dampen vibrations, thereby preventing secondary fiber fracture. One end of a 100 mm long fiber was taped to a piece of polyethylene film. The exposed section of fiber was coated with a water-soluble grease (Phynal, Reliance Glass Works, Bensenville, IL). The fiber section was long enough so that it protruded ~20 mm past the end of the film. The polyethylene film with fiber attached was gripped at the tape location and the protruding end of the fiber was gripped with a rubber-faced clamp grip as for standard tensile testing. The overall gauge length of fiber was 75 mm for fractography testing. After fracture, the grease was removed from the fiber by two soaks in deionized water,

followed by an ethanol rinse. The matched broken end pairs were mounted vertically on scanning electron microscopy (SEM) stubs for examination.

High temperature fiber strength testing was performed vertically using a slotted furnace with a hot zone 20 mm long. Fibers were loaded into the test frame, the hot furnace was slid around the fiber and equilibrated for 90 seconds before beginning the test. For strand testing, the overall gauge length was 250 mm and the strain rate was 12.5 mm/sec. For single filament testing, the overall gauge length was 280 mm and the strain rate was 0.68 mm/minute.

Creep testing was performed using a single filament, dead load testing system to provide an accurate and consistent load. Sample elongation was measured with a Zygo[®] laser extensometer (Model 1101, Zygo Corp, Middlefield, CT). The creep system used a resistance-heated, three zone alumina tube furnace with Nichrome heating elements. Hot zone temperature was accurate to within 3°C of the setpoint over the entire 106 mm gauge length. The creep rate was assumed to be uniform over this gauge length. Details of this creep system have been described previously².

Results

Table 1 summarizes the properties of Nextel 610 fiber, Nextel 650 fiber and Nextel 720 fiber. Nextel 610 fiber is >99% pure α -Al₂O₃ with a grain size of ~0.1 μ m. Nextel 610 has properties expected of an alumina fiber; the elastic modulus and density are slightly below theoretical (400 GPa, 3.98 g/cm³), reflecting a small amount of porosity. Thermal expansion is very close to measured values for monolithic alumina.

Nextel 650 fiber has the composition $\text{Al}_2\text{O}_3 + 10\% \text{ZrO}_2 + 1\% \text{Y}_2\text{O}_3$. The microstructure of Nextel 650 fiber consists primarily of $0.1 \mu\text{m}$ $\alpha\text{-Al}_2\text{O}_3$ grains; ZrO_2 is present as 5-30 nm grains on both grain boundaries and within alumina grains⁸. The key additive in Nextel 650 fibers is Y_2O_3 , which is added to reduce creep rate. ZrO_2 additions are used to reduce grain growth, which is accelerated by Y_2O_3 doping. Zirconia is stabilized by Y_2O_3 in the cubic phase. The addition of ZrO_2 had only a minor effect on creep rate for either rare earth doped or undoped alumina fibers. Density and thermal expansion have not yet been directly measured, but are higher than Nextel 610 fiber due to the present of 10% ZrO_2 . Elastic modulus was measured to be slightly lower than Nextel 610 fibers, as expected since ZrO_2 has lower modulus than Al_2O_3 . Nextel 720 fiber contains 15% SiO_2 in the form of mullite; volume calculations indicate that mullite comprises 55-60% of the fiber volume. The high content of mullite lowers density and thermal expansion by 13% and 30%, respectively. These can be significant advantages for aerospace and thermally loaded applications. The microstructure of Nextel 720 fiber has been described in more detail elsewhere¹⁴.

Development of High Fiber Strength

A major application of Nextel 610 fiber is to strengthen and stiffen aluminum metal composites; therefore, high strength is a primary requirement. The high strength of Nextel 610 fibers is the result of intensive microstructural design and process development efforts. Among oxide ceramics, Al_2O_3 is generally considered the most desirable structural material. Al_2O_3 has excellent fracture toughness, high elastic modulus, and very good thermochemical stability. However, the fabrication of Al_2O_3 in

fiber form is not straightforward. The stable α form of Al_2O_3 has a low volumetric nucleation density, which leads to large grain size¹⁵. In addition to large grains, crystallization often leads to high levels of porosity which inhibit sintering. Thus, control over the nucleation process during crystallization is essential if the fine grain sizes required for high strength are to be achieved. In Nextel 610 fiber, nucleation agents are used to produce a uniform, high-density microstructure with a grain size of 0.1 μm .

In addition to small grain size, other defects and flaws must be minimized by careful fiber processing. The sol/gel process in combination with effective nucleation agents is uniquely suited to the preparation of such extremely fine-grained and homogeneous fiber microstructures. However, achieving this level of control is difficult. Figure 1 shows the mean strength of Nextel 610 fibers produced during each year since 1989. Initial versions of Nextel 610 had strength below 2 GPa. During the late 80's and early 90's, large internal programs to develop first titanium and later, aluminum composites reinforced with Nextel 610 were performed^{16,1}. Focussed efforts were carried out to increase the strength of Nextel 610 fiber to greater than a target of 2.8 GPa. As shown in Figure 1, these efforts were successful over time in increasing strength to 3.3 GPa. Keys to this effort were the development of improved nucleation agents, intensive efforts to reduce the level of internal particulate defects, and careful control of fiber spinning and heat treatment to prevent fiber damage during processing.

During fiber development, fractography testing was performed to identify fracture-causing defects in Nextel 610 fibers. Figures 2, 3 and 4 are scanning electron micrographs of fractured surfaces of Nextel 610 fibers generated during fractography

testing. The mean strength of the sample of 16 fibers tested was 3.27 GPa. Fourteen of the 16 fibers fractured at defects at the fiber surface. A high proportion of surface fracture origins in Nextel 610 fibers has also been reported elsewhere¹⁷. Figure 2 shows a fiber that fractured at a weld lines running down the length of the fiber surface. The weld line resulted from contact with a neighboring fiber during processing. Fracture occurred at one of the weld lines at 3.85 GPa. The weld line is 0.5 μm in width and 0.25 μm in depth. The fracture surface morphology has an indistinct mirror-mist-hackle appearance. Within ~ 1 μm of the fracture origin, the fracture surface is relatively smooth; outside of that “mirror” region, the fracture surface becomes textured, and striations lead away from the fracture origin. Figure 3 shows a fiber that broke at a surface scratch 0.7 μm wide and 0.5 μm in depth (3.38 GPa). The surface scratch was probably caused by mechanical abrasion in the green (unfired) state. A fiber which broke at an internal, round, smooth pore 1.3 μm in size is shown in Figure 4 (3.74 GPa). This pore was likely caused by an air bubble in the sol/gel precursor used to spin the fiber.

As brittle ceramics, the strength of Al_2O_3 fibers is controlled by the Griffith fracture criterion:

$$\sigma = K_{Ic}/m(\pi c)^{1/2} \quad (4)$$

where c is flaw size and m is a geometrical factor. In Al_2O_3 , the fracture toughness K_{Ic} is near 2.8. For a semicircular surface flaw, $m = \pi/2$, or 0.64¹⁸. Figure 5 shows the Griffith strength prediction for Al_2O_3 as a function of flaw size. In order to achieve >3 GPa strength in alumina fibers, a flaw size well below 1 μm is necessary. Figure 5 also shows the strength of Nextel 610 fibers during fractography testing as a function of

measured defect size. In general, the width of surface flaws was twice their depth, i.e., the flaws are roughly semicircular (for the diagram in Fig. 5, $a = b$). In Fig. 5, measured flaw size was plotted as the depth, a , of the flaw. As predicted by the Griffith equation, larger defects generally correlated with lower fiber strength. However, for surface flaws, measured fiber strength was somewhat less than predicted by Eq. 4. This may indicate that the fracture toughness of Nextel 610 fibers is less than larger-grained alumina; large-grained alumina is known to have higher fracture toughness due to crack-wake effects that are unlikely to be operative in a ceramic fiber. However, note that the extremely small size of the defects and the polycrystalline nature of the fiber creates some uncertainty about precise location of flaw boundaries. For instance, there may be some extension of the crack over one or two grains prior to fracture, effectively increasing the size of the flaws. The two fibers that fractured at round pores had higher strength than the Griffith prediction (for round pores, flaw size, c , was pore diameter divided by 2). The smooth, round internal surface of these pores minimizes the stress concentration relative to other types of defects; these pores are not sharp flaws as required by Eq. 4.

Weibull Statistics of Fiber Strength

To determine Weibull modulus, 369 fibers from a single sample of Nextel 610 fibers were tested at 25 mm gauge length. Figure 6 shows the data plotted as a Weibull plot. Two methods were used for data analysis. In one data set, fiber strength was calculated using breaking load divided by the cross-sectional area, as determined from individual diameter measurements for each broken fiber. In the other data set, the mean

measured diameter of 11.98 μm was used to calculate breaking strength from the individual breaking load measurements. The correlation of the best-fit line to both data sets is only fair. The fiber fracture data deviates above the best-fit line for high strength fibers and below the line for low strength fibers for both sets of data. The cause of the poor fit appears to be an overly large effect on the least-squares fit of weakest 4 fibers at the end of the distribution. If the 4 lowest data points are removed, the fit improves greatly, and the Weibull modulus is increased $\sim 10\%$. Other methods of curve fitting, e.g., maximum likelihood estimator¹⁹, have been shown to be more accurate than the least-squares method used for this data, but these methods were not applied in this study. The Weibull modulus was determined to be 11.2 for the data set with individual diameter measurements, and 9.7 for the data set using mean diameter. The lower Weibull modulus of fiber strengths calculated using mean diameter is expected; the calculated distribution will be created by the overlap of the “true” dispersion of strength and the dispersion of fiber volume created by diameter variability. For instance, larger diameter fibers will, on average, have higher breaking loads. If mean diameter is used, then these fibers will have erroneously high calculated strength. Conversely, smaller diameter fibers will have erroneously low calculated strength. This will broaden the calculated distribution of fiber strength relative to the “true” distribution and therefore the Weibull modulus will be lowered. This effect has been modeled recently by Lara-Curzio²⁰. For the data in Figure 6 (COV of diameter of (1.8%), Lara-Curzio predicts a $\sim 5\%$ reduction in measured Weibull modulus. For more typical diameter distribution in Nextel 610 fibers (5%)²¹, the predicted drop in measured Weibull modulus with the use of mean diameter is 10%. These predictions are somewhat less than measured reduction

from 11.2 to 9.7 (15%), but are reasonable given uncertainties in fiber diameter measurement on the sub-micrometer level²².

Figure 7 is a Weibull plot that compares the strength of Nextel 610 fibers, Nextel 650 fibers and Nextel 720 fibers. Data for Nextel 610 and 720 fibers were taken from entire production lots in late 1999 and early 2000, respectively. Sets of 10 fibers were tested at periodic intervals through one production run. These sets were combined into a single population for analysis. A total of 140 Nextel 610 fibers and 120 Nextel 720 fibers were tested. Nextel 650 is currently in early stages of development and less data is available. Two sets of 10 fiber breaks were combined for this analysis. As described above, fiber strength was calculated using mean diameters; thus, the Weibull values should be conservative by 10% or more.

The strength of the fibers increased from 1.98 GPa for Nextel 720 fibers to 2.60 GPa for Nextel 650 fibers to 3.40 GPa for Nextel 610 fibers. The Weibull modulus was 10.1 for Nextel 610, ~30% higher than for either Nextel 650 or Nextel 720 fibers, which had Weibull moduli of 6.8 and 7.6, respectively. These values are very similar to those reported previously for earlier lots of Nextel 610 and 720 fibers²¹. The Weibull modulus for Nextel 610 fibers is also similar to the other lot of fibers tested in Figure 6. The expected fit to the linear Weibull relationship is good, though both Nextel 610 and 720 fibers show a deviation toward high strengths at both ends of the probability range. The reason for the higher Weibull modulus for Nextel 610 fiber relative to the other fibers is not clear. One possibility is that the single-phase alumina microstructure of Nextel 610 fiber provides increased microstructural and therefore flaw homogeneity relative to the other fibers, which have multiple phases. Alternately, microscopy and fractography

work has identified weld lines as critical defects in both Nextel 650 and 720 fibers; the different fiber compositions may have different intrinsic propensity toward inter-filament adhesion via sintering, which could lead to different flaw populations.

Figure 8 shows a log-log plot of single filament strength for Nextel 610, 650 and 720 fibers as a function of gauge length in the range 25 mm – 254 mm. Ten filaments were tested at each gauge length for each type of fiber. The strength of these samples at 25 mm gauge length was 3.49 GPa, 2.75 GPa and 2.24 GPa, respectively, for Nextel 610, 650 and 720 fibers. Fiber strength was determined using mean diameters calculated from fiber denier of 11.52 μm , 11.22 μm , and 12.34 μm , as discussed above. As predicted by Equation 3, fiber strength decreased as gauge length increased. The Weibull modulus determined from the slope of the best-fit lines was 9.7, 7.3 and 7.1 for Nextel 610, 650 and 720 fibers, respectively. These values agree very well with data from Figure 7 using the statistics of fracture at a single gauge length. The agreement is within 7% for all three fibers. Thus, the results are consistent with a single population of flaws distributed uniformly throughout the fiber bundles. Previous results had indicated a higher Weibull modulus for gauge length measurements²¹. The reason for the difference is not clear; these measurements span a large range of gauge lengths than the previous study.

High Temperature Fiber Properties

High temperature fiber strength was measured in two ways. The strength of multifilament rovings was measured for all six commercially available Nextel fibers.

For the fibers most commonly used for high temperature ceramic composites, Nextel 610, 650 and 720 fibers, high temperature single filament testing was also performed.

Figure 9 compares the relative high temperature multi-filament strand or roving strength of all available Nextel fibers. Since the number and diameter of the fibers is different for each type of fiber, the data is presented as a percentage of room temperature strength. The room temperature strength was measured on fibers that had the sizing removed by heat cleaning for 5 minutes at 700°C. All fibers retained >90% of their room temperature strength at 800°C. Using a criterion of 70% strength retention, the temperature capability of the fibers is given in Table 2. Nextel 312 fiber has the lowest temperature capability. Creep has been observed in Nextel 312 fiber at 600°C: a large component of Nextel 312 fiber is amorphous and subject to viscous deformation under load. Nextel 440 fiber, which has lower B₂O₃ content, has improved temperature capability. Nextel 550 fiber, which is B₂O₃-free, has strength and creep resistance similar to Nextel 610 fiber. Both maintained 70% of room temperature strength at 1300C. The high temperature strength of Nextel 650 fiber is 100 °C better than Nextel 610 fiber. Nextel 720 fiber showed no degradation in strand strength up to maximum temperature of 1400°C used in this testing. Of the fibers most commonly used for high temperature composite applications, Nextel 610 fibers retained 60% of their RT strength at 1300C, Nextel 650 fibers 80%, and Nextel 720 fibers, 90%.

Figure 10 shows the high temperature single filament strength of the three composite fibers, Nextel 610, 650, and 720 fibers. The samples of fiber tested were the same as those used for gauge length testing. The relative single filament strength retention of the 3 fibers was similar to the strand tests. Nextel 610 fibers retained 70%

of room temperature strength up to 1000°C, Nextel 650 fibers to 1200°C and Nextel 720 fibers to 1300°C. Overall, the strand and single filament data suggests an improvement in temperature capability for Nextel 650 fibers relative to Nextel 610 fibers of 100°C; Nextel 720 fiber has a temperature capability a further 100°C higher than Nextel 650 fiber. The relative high temperature strengths of these fibers correlated well with relative creep rates (Figure 11).

All three composite fibers retained strength to ~200°C higher temperature in strand testing than single filament testing. The reason for this is strain rate. The strain rate for strand testing (0.05/sec) was 3 orders of magnitude higher than for the single filament testing (4×10^{-5} /sec). A reduction in high temperature strength is expected at temperatures where inelastic deformation mechanisms (i.e., creep) are active, leading to the extension of existing critical flaws and to the formation of new cracks and other flaws. At high strain rates, these time-dependent stress rupture phenomena are minimized and strength is higher. For instance, at 1100°C, the strength of Nextel 610 fiber was 70% of the room temperature strength of 3.47 GPa, or ~2.5 GPa.

Extrapolation of the creep data in Figure 11 for Nextel 610 fiber at 1100°C indicates that the expected creep rate at 2 GPa stress is greater than the strain rate for single filament tensile testing (4×10^{-5} /sec). Conversely, for roving testing at the much slower rate of 0.05/sec, significant deformation would be expected only at much higher temperature. In fact, stress-strain plots for Nextel 610 single filaments at 1200°C and higher were consistent with a large degree of inelastic deformation. For Nextel 650 fibers, a large amount of inelastic deformation was observed only at 1300°C and for Nextel 720 fibers, 1400°C.

Figure 11 compares the creep rate at 1100C of Nextel 610 fiber, Nextel 650 fiber, and Nextel 720 fiber. The creep rate of Nextel 720 fiber at 1200C is also shown. The creep rate decreased in the order Nextel 610 fiber > Nextel 650 fiber > Nextel 720 fiber. The difference in creep rate was a factor of 10-100 times between each type of fiber. At a stress of 100 MPa, the strain rate of Nextel 610 was 1×10^{-6} /sec, Nextel 650 fiber, 1×10^{-8} /sec, and Nextel 720, 1×10^{-10} /sec. This magnitude of difference increases fiber temperature capability by ~100C. Creep data at 1200C for Nextel 720 fiber are also included in Figure 11. The creep rate of Nextel 720 fiber at 1200C is very similar to Nextel 650 fiber at 1100C. Using a criterion of 69 MPa stress, 1100 C and a 1% maximum strain in 1000 hours, Nextel 610 fibers have a temperature capability of ~1000C. Using the same criterion, the temperature capability for Nextel 650 and Nextel 720 fiber is 1080C and 1150C, respectively. The stress exponent for both Nextel 610 and 720 fibers was very close to 3. The stress dependence of creep for Nextel 650 fiber was 1.8, less than the other fibers. The reason for this is not known; Harmer¹² reported no change in stress dependence with Y³⁺ doping.

Nextel 720 fiber has the best creep performance of any commercially available polycrystalline oxide fiber. However, further reductions in creep of oxide fibers are possible. For instance, yttrium aluminum garnet (YAG) fibers are the focus of a current developmental program at 3M. YAG is the most creep-resistant polycrystalline oxide⁹ and also has very slow grain growth kinetics at high temperature, suggesting that YAG fibers would be an ideal fiber for high temperature composites. Short lengths of YAG fibers have been produced in the laboratory with 700 MPa strength. Bend stress relaxation measurements indicate that these fibers would have a use temperature 50C

higher than Nextel 720 fiber. Figure 12 shows a YAG fiber heat treated to 1200C that has a grain size of 0.1 μm . Although not visible by scanning electron microscopy, this fiber contains a substantial amount of porosity. Elimination of this porosity would be expected to reduce creep rates further.

Conclusions

Nextel 610 fiber has high strength (3.3 GPa), Weibull modulus (11) and excellent thermochemical stability provided by its ultra-fine grained, single phase $\alpha\text{-Al}_2\text{O}_3$ microstructure. It maintains excellent high temperature strength and resists creep temperatures up to 1000C. Nextel 720 fiber comprises a majority of large, 0.5 μm , creep-resistant mullite grains; as a result, Nextel 720 fiber has 150C-200C higher temperature capability than Nextel 610 fiber as measured by high temperature strength and creep testing. It is suitable for load bearing applications at temperatures as high as 1200C. The strength (2.0 GPa) and Weibull modulus (7) of Nextel 720 fiber is less than Nextel 610 fiber. Nextel 650 fiber has properties intermediate between Nextel 610 and 720 fibers. Good creep resistance is provided by Y_2O_3 doping; good strength and chemical stability is provided by a fine, uniform, high alumina microstructure. Nextel 650 fiber has a strength of 2.5 GPa, a Weibull modulus of 7, and maintains strength and creep resistance as high as 1100C. Continued improvements in the strength and high temperature performance of oxide fibers the focus of on-going research at 3M.

Acknowledgements

The assistance of Joe Schneider, Sandy Deppe and Ruth Ann Williams at 3M and Rich Goettler of McDermott Technology in single filament testing is greatly appreciated. The efforts of Jim Reimer for creep measurements and Steve Pittman for SEM microscopy are also acknowledged. Garnet fiber work was supported by DOE under contract DE-FC02-92CE40945. Such support does not constitute an endorsement by DOE of the views expressed in the article.

References

1. Deve, H. E. & McCullough, C., Continuous-fiber reinforced Al composites: a new generation J. of Met., 1995, **47**, 33-37.
2. Wilson, D. M., Lieder, S. L. & Lueneburg, D. C., Microstructure and high temperature properties of Nextel 720 fibers. Cer. Eng. Sci. Proc., 1995, **16**, 1005-1014.
3. Wilson, D. M., Lieder, S. L. & Lueneburg, D. C., Materials Research Society Symposium Proceedings, Vol. 350, Intermetallic Matrix Composites III, edited by J.A. Graves, R.R. Bowman, and J.J. Lewandowski (Mat. Res. Soc., Pittsburg, PA, 1994) pp. 89-98.
4. Goering, J. & Schneider, H., Creep and subcritical crack growth of NextelTM 720 aluminosilicate fibers as received and after heat treatment at 1300°C. Cer. Eng. Sci. Proc., 1997, **18**, 95-102.
5. Kramb, V. A., John, R. & Zawada, L. P., Notched fracture behavior of an oxide/oxide ceramic-matrix composite. J. Am. Ceram. Soc., 1999, **82**, 3087-96.

6. Levi, C. G., Yang, J. Y. Dalgleish, B. J. Zok, F. W. & Evans, A. G., Processing and performance of an all-oxide ceramic composite. *J. Am. Ceram. Soc.*, 1998, **81**, 2077-86.
7. Heathcote, J. A., Gong, X-Y. Ramamurty, U. & Zok, F. W., In-plane mechanical properties of all-oxide ceramic composite. *J. Am. Ceram. Soc.*, 1999, **82**, 2721-30.
8. Wilson, D. M. & Visser, L. R., Nextel™ 650 Ceramic Oxide Fiber: New Alumina-Based Fiber for High Temperature Composite Reinforcement. *Cer. Eng. Sci. Proc.*, Vol. 21, to be published in 2000.
9. French, J. Zhao, M. Harmer, H. Chan & G. Miller, Creep of duplex microstructures. *J. Am. Ceram. Soc.*, 1994, **77**, 2857-65.
10. Sato, E. & Carry, C. , Yttria doping and sintering of submicrometer-grained α -Al₂O₃. *J. Am. Ceram. Soc.*, 1996, **79**, 2156-60.
11. Pint, B. A., Garrat-Reed, A. J. & Hobbs, L. W., Possible role of the oxygen potential in enhancing diffusion of foreign ions on α -Al₂O₃ grain boundaries. *J. Am. Ceram. Soc.*, 1998, **81**, 305-14.
12. Bruley, J. , Cho, J. , Chan, H. M. , Harmer, M. P. & Rickman, J. M., Scanning transmission electron microscopy analysis of grain boundaries in creep-resistant yttrium- and lanthanum-doped alumina microstructures. *J. Am. Ceram. Soc.*, 1999, **82**, 2865-70.
13. Van Der Zwaag, S., The concept of filament strength and the Weibull modulus. *J. Test Eval.*, 1989, **17**, 292-298.

14. Hay, R. S., Boakye, E. E., Petry, M. D., Berta, Y. Von Lehnden, K., & Welch, J., Grain growth and tensile strength of 3M Nextel 720™ after thermal exposure. Cer. Eng. Sci. Proc., 1999, **20**, 153-163.
15. Kumagai, M. & Messing, G. L., “Controlled transformation and sintering of a boehmite sol-gel by α -alumina seeding”. J. Am. Ceram. Soc., 1985, **68**, 500-505.
16. Deve, H. E. & McCullough, C., Fiber coating performance in TiAl. Materials Research Society Symposium Proceedings, Vol. 350, Intermetallic Matrix Composites III, edited by J. A. Graves, R.R. Bowman, and J.J. Lewandowski (Mat. Res. Soc., Pittsburg, PA, 1994) pp. 119-124.
17. Cantonwine, P. E., Processing and properties of an alumina composite fiber. Ph.D. Thesis, 1999, University of Virginia.
18. Lawn, B. R. & Wilshaw, T. R., *Fracture of Brittle Solids*, Cambridge Univ. Press, Cambridge, 1975, pp. 58-61.
19. Sonderman, D., Jakus, K., Ritter, J. E., Yuhaski, S. & Service, T. H., Maximum likelihood estimation techniques for concurrent flaw subpopulations. J. Mat. Sci., 1985, **20**, 207-212.
20. Lara-Curzio, E. & Russ, C. M., On the relationship between the parameters of the distributions of fiber diameters, breaking loads, and fiber strengths. J. Mat. Sci. Lett., 1999, **18**, 2041-44.
21. Wilson, D. M., Statistical strength of Nextel™ 610 and Nextel™ 720 fibers. J. Mat. Sci., 1997, **32**, 2535-42.

22. Hurst, J. B., Hong, W. S., Gambone, M. L., Porter J. R. “ASTM Single Fiber Room Temperature Test Standard Development”, 1998. Am. Soc. Mech. Eng., paper 98-GT-567, presented at International Gas Turbine & Aeroengine Congress, Stockholm, Sweden.

Table 1. Properties of Nextel 610, 650, and 720 Ceramic Fibers

Property	Units	Nextel™ 610	Nextel™ 650	Nextel™ 720
Chemical Composition	wt. %	>99 Al ₂ O ₃	89 Al ₂ O ₃ 10 ZrO ₂ 1 Y ₂ O ₃	85 Al ₂ O ₃ 15 SiO ₂
Crystal Phases		α-Al ₂ O ₃	α-Al ₂ O ₃ + cubic ZrO ₂	α-Al ₂ O ₃ + mullite
Tensile Strength (25.4 mm gauge)	GPa	3.3	2.5	2.1
Tensile Modulus	GPa	373	358	260
Density	g/cc	3.9	4.1	3.4
Thermal Expansion (100-1100°C)	ppm/ °C	7.9	8.0	6.0
Max Use Temperature (1% strain/ 69 MPa/1000 hr)	°C	1000C	1080C	1150C
Roving Denier: Filament Count		1500: 380-420 3000: 740-780 10000: 2500- 2600	3000: 740 780	1500: 380-420 3000: 740-780

Table 2. Roving Strength Maximum Temperature Limit (70% Strength Retention)

Fiber	Roving Strength Maximum Temperature Limit*
Nextel 312	950°C
Nextel 440	1200°C
Nextel 550	1300°C
Nextel 610	1300°C
Nextel 650	1400°C
Nextel 720	>1400°C

* Strain rate = 12.5 mm/min

Figure Captions

- Figure 1. Single filament strength of Nextel 610 has steadily increased to over 3 GPa (data points represent mean fiber strength for each year).
- Figure 2. SEM of fracture surface of Nextel 610 fiber from fractography testing. The fiber broke at a stress of 3.27 GPa at a weld line 0.25 μm in depth caused by inter-filament adhesion during processing. Bar = 1 μm .
- Figure 3. SEM of fracture surface of Nextel 610 fiber from fractography testing. The fiber broke at a stress of 3.83 GPa at a surface scratch 0.5 μm in depth. Bar = 1 μm .
- Figure 4. SEM of fracture surface of Nextel 610 fiber from fractography testing. The fiber broke at a stress of 3.38 GPa at a 1.3 μm round, internal pore. Bar = 1 μm .
- Figure 5. Comparison of measured flaw size with the Griffith strength prediction for Al_2O_3 fibers ($K_{Ic} = 2.8$) with semicircular surface flaws. Flaw size must be well below 1 μm to achieve 3 GPa strength. Measured flaw size, a , was slightly less than the predicted strength for surface flaws, but above the prediction for round, internal pores.
- Figure 6. Weibull plot of fracture probability as a function of failure stress using a) measured individual filament diameters and b) calculated mean diameter of 11.98 μm . Using mean diameter, Weibull modulus was 15% less.
- Figure 7. Weibull plot of fracture probability. The strength of Nextel 610, 650 and 720 fibers was 1.98 GPa, 2.60 GPa, and 3.40 GPa, respectively, and the Weibull moduli were 10.1, 6.8 and 7.6.
- Figure 8. Log-log plot of failure strength of Nextel 610, 650 and 720 fibers as a function of gauge length. Weibull modulus is equal to the inverse of the slope of the best-fit lines. The Weibull moduli of Nextel 610, 650 and 720 fibers were 9.7, 7.3 and 7.1, respectively.
- Figure 9. Comparison of relative tensile strength retention of multi-filament strands of Nextel 312, 440, 550, 610, 650 and 720 fibers at elevated temperature.
- Figure 10. Comparison of relative tensile strength retention of single filaments of Nextel 610, 650 and 720 fibers at elevated temperature. Nextel 610 fibers retained 70% of room temperature strength up to 1000°C, Nextel 650 fibers to 1200°C and Nextel 720 fibers to 1300°C.
- Figure 11. Comparative creep rate of Nextel fibers at 1100C as a function of stress. The creep rate of Nextel 610 fibers was 1 to 2 orders of magnitude higher than Nextel 650 fiber. The creep rate of Nextel 720 fiber was a further 1-2 orders of magnitude lower.
- Figure 12. Scanning electron micrograph of YAG fiber heat treated at 1200°C. Fiber grain size is near 0.1 μm . Bar = 5 μm .

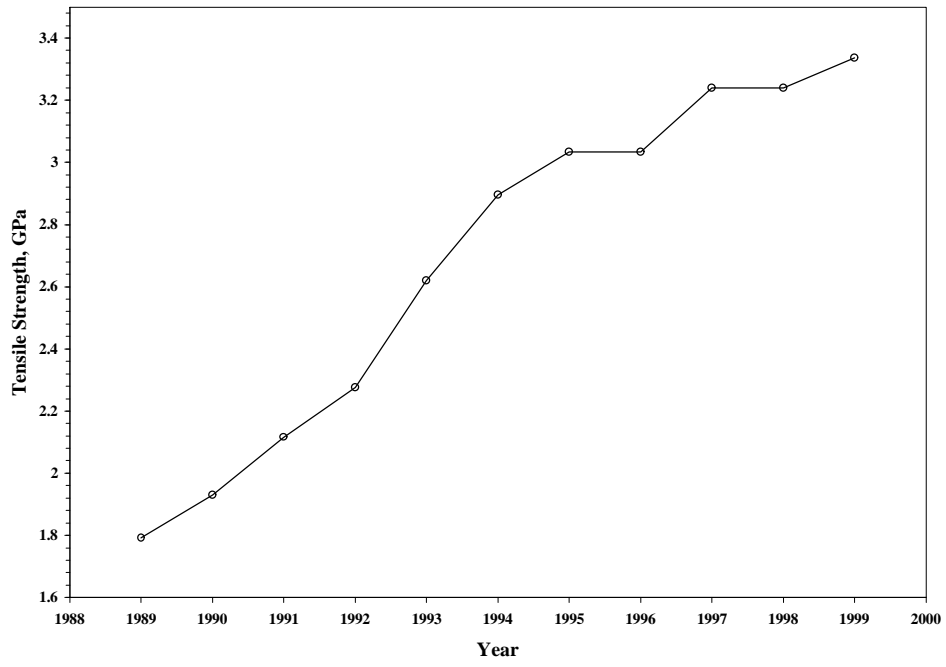


Figure 1.

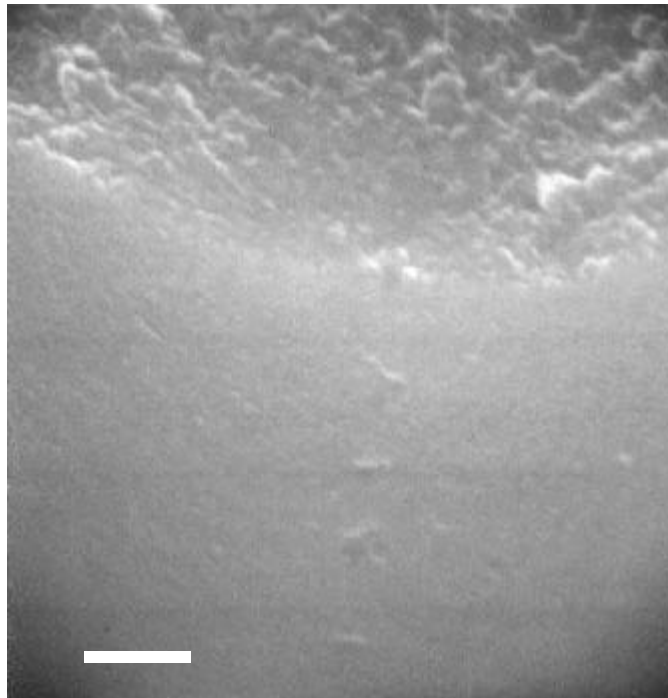


Figure 2.

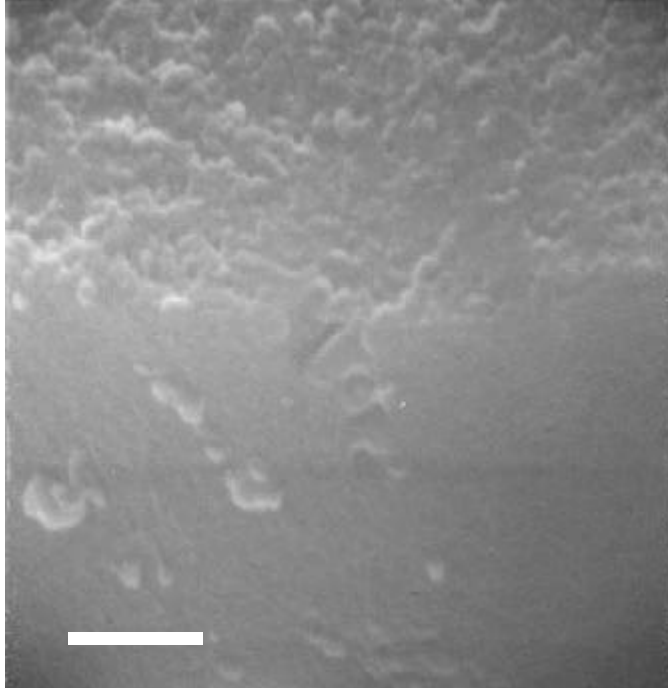


Figure 3

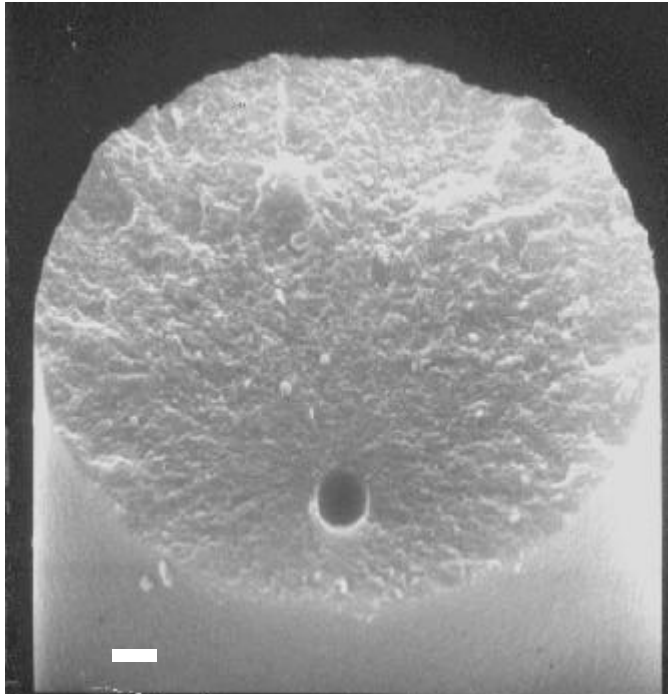


Figure 4

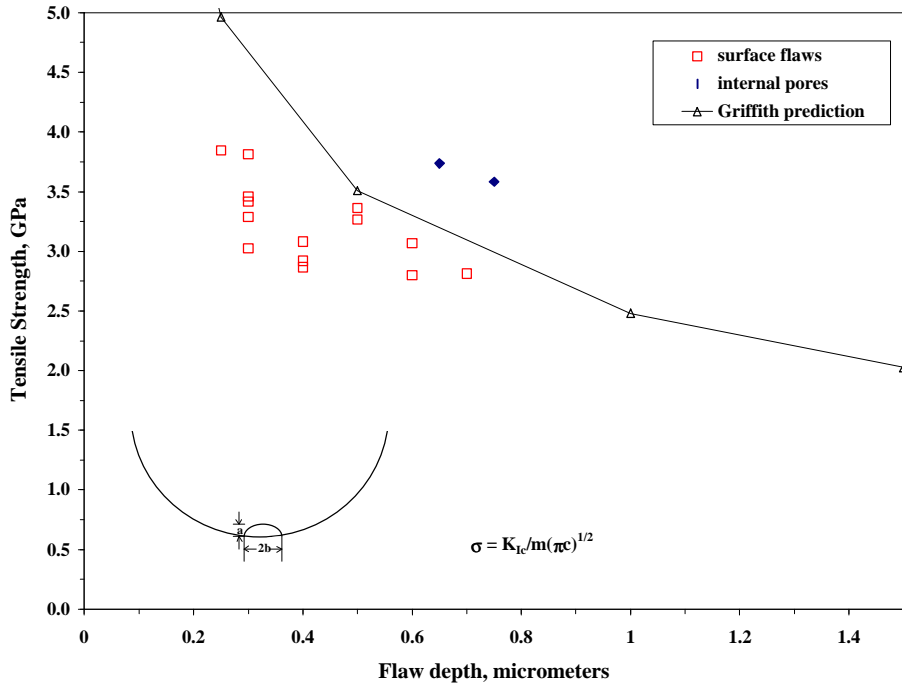


Figure 5

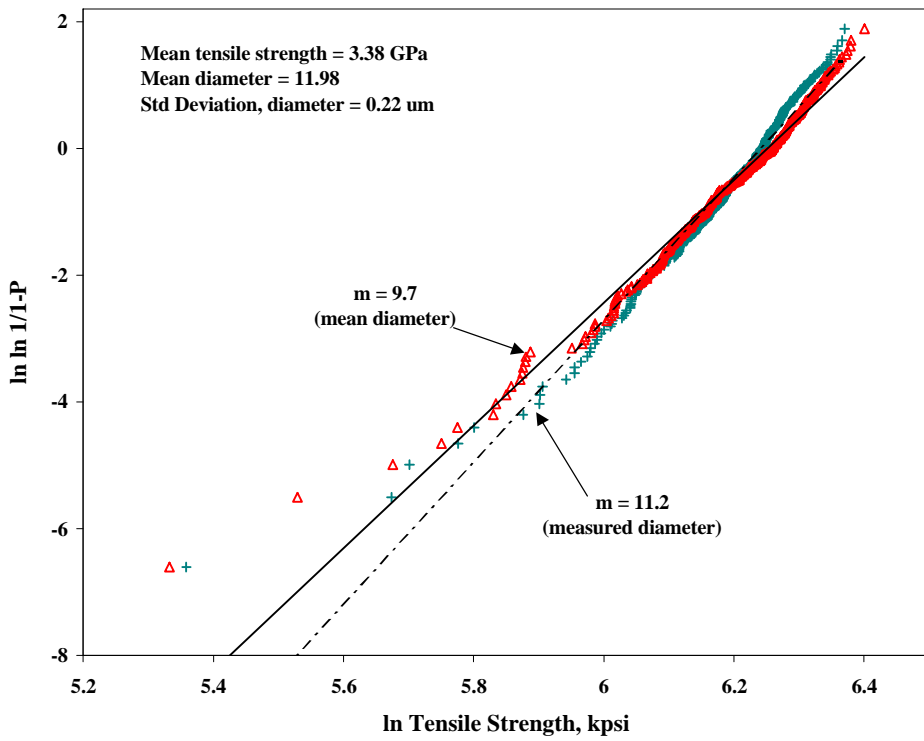


Figure 6

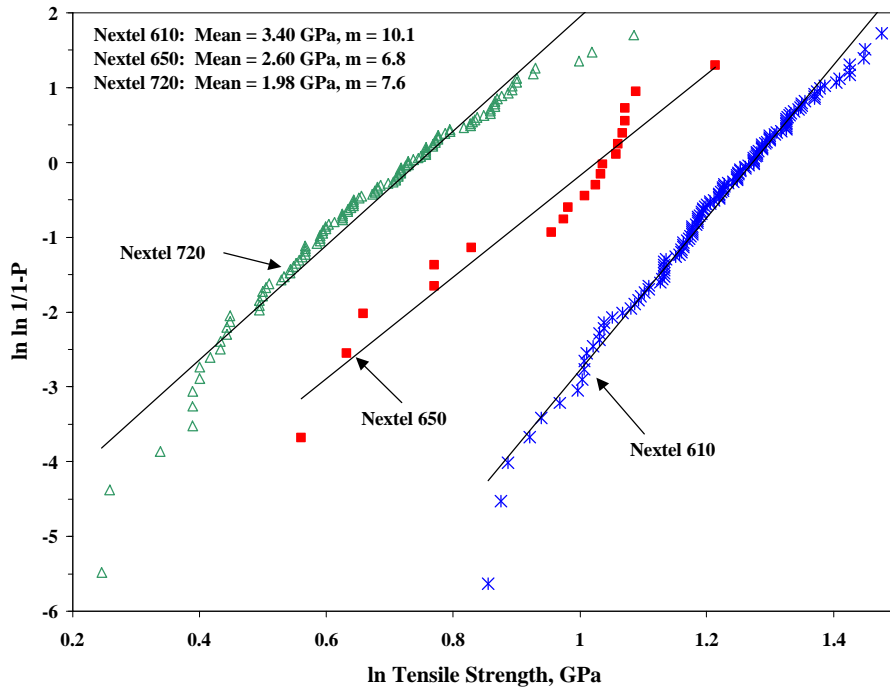


Figure 7

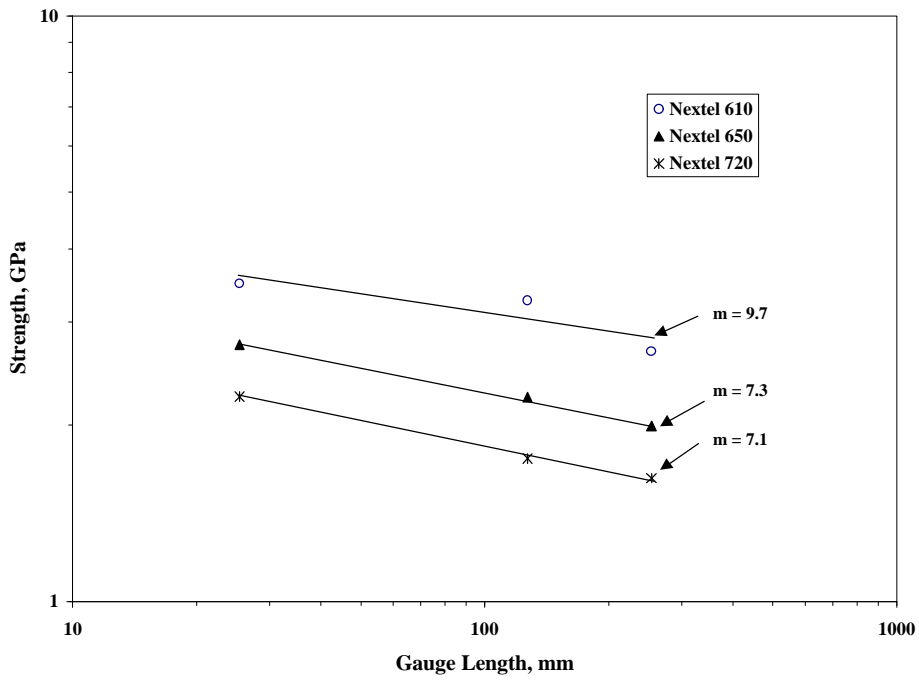


Figure 8

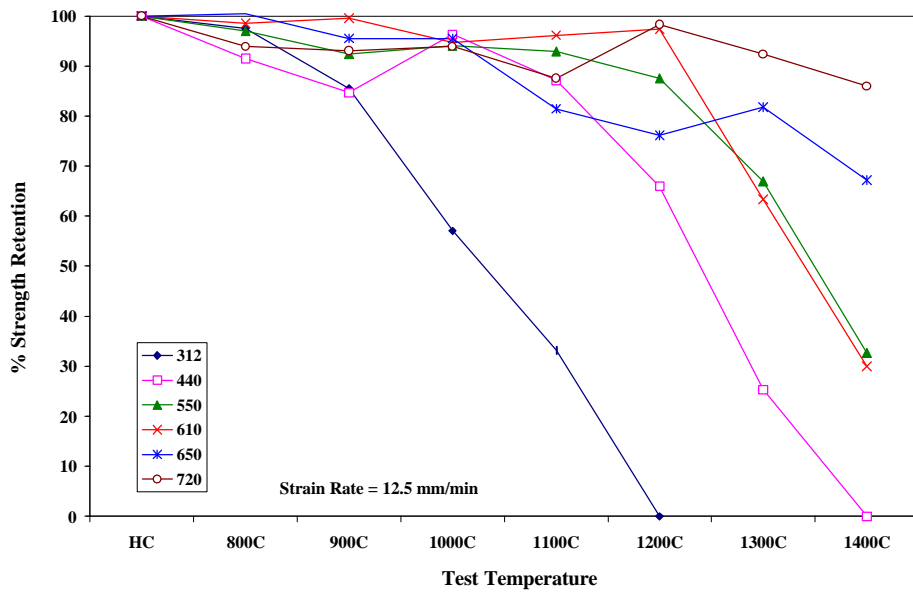


Figure 9

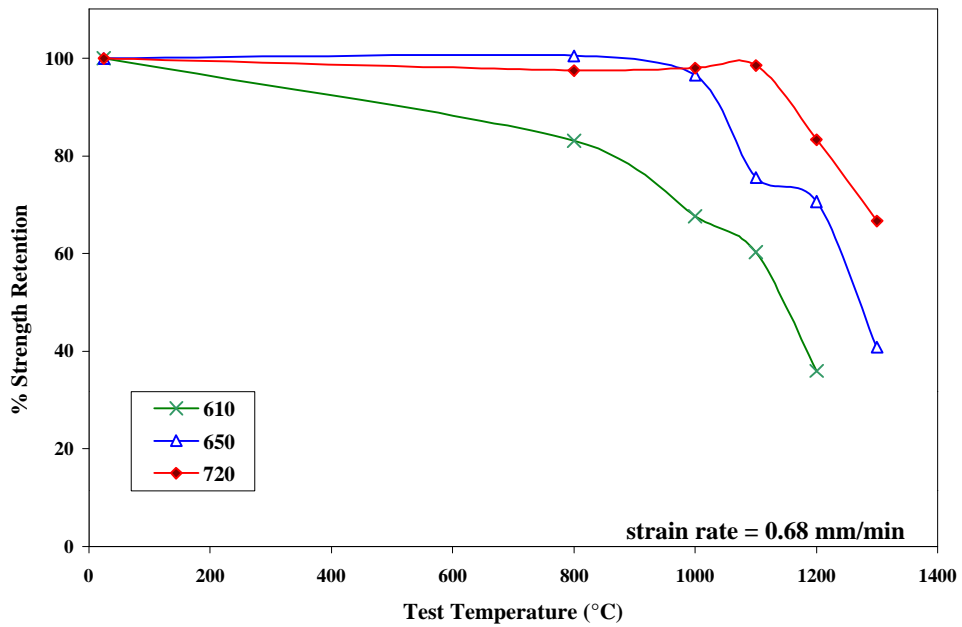


Figure 10

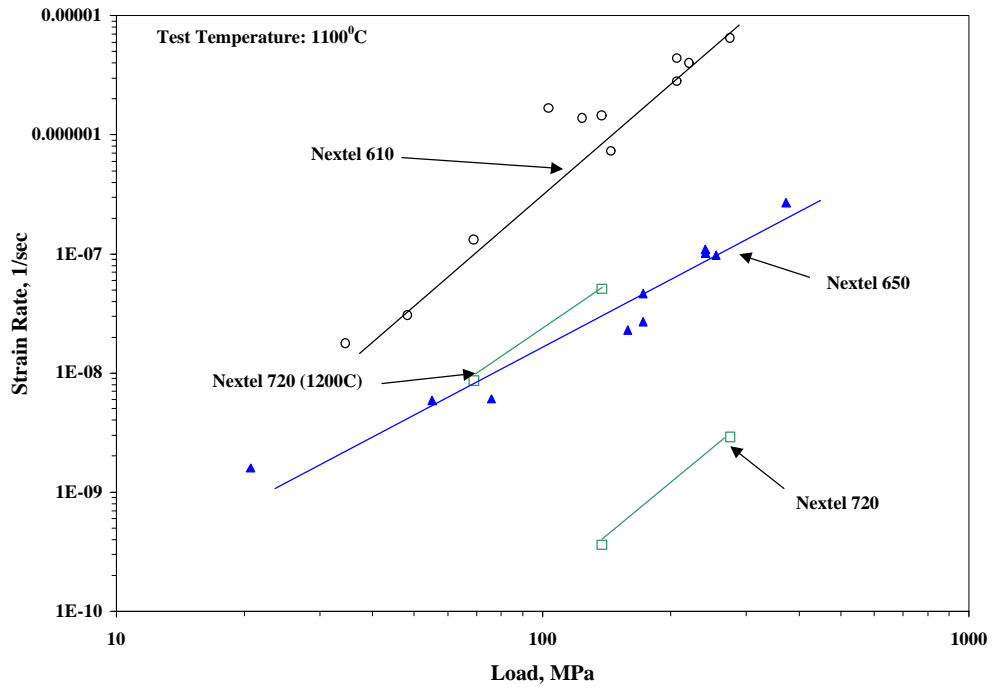


Figure 11

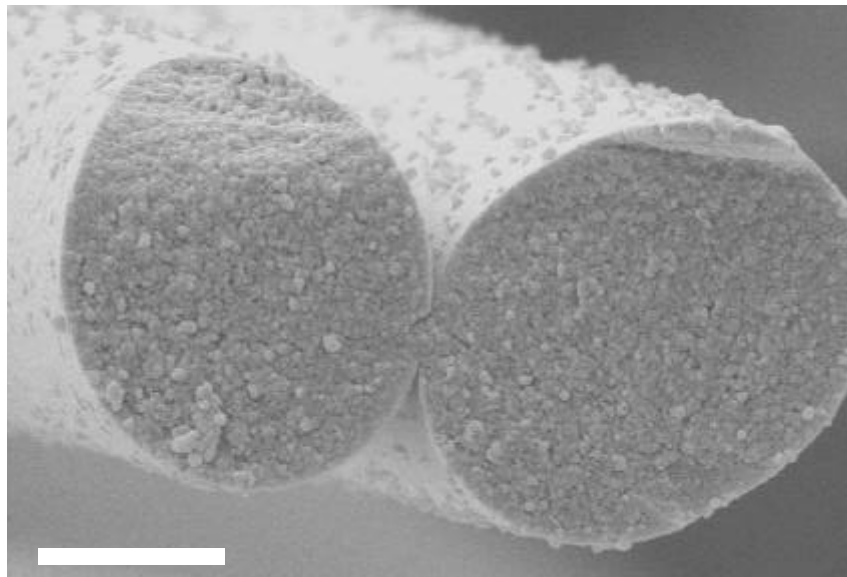


Figure 12